International Journal of Greenhouse Gas Control 69 (2018) 72–80

Contents lists available at ScienceDirect

International Journal of Greenhouse Gas Control

journal homepage: www.elsevier.com/locate/ijggc

Assessment of two-phase flow on the chemical alteration and sealing of leakage pathways in cemented wellbores

Jaisree Iyer[a,*], Stuart D.C. Walsh[b], Yue Hao[a], Susan A. Carroll[a]

[a] Lawrence Livermore National Laboratory, 7000 East Avenue, Livermore, CA 94550, USA
[b] University of New South Wales, UNSW Sydney, 2052 NSW, Australia

ARTICLE INFO

Keywords:
Carbon storage
Two-phase flow
Wellbore integrity
Cement-CO_2 reactions

ABSTRACT

Wellbore leakage tops the list of perceived risks to the long-term geologic storage of CO_2, because wells provide a direct path between the CO_2 storage reservoir and the atmosphere. In this paper, we have coupled a two-phase flow model with our original framework that combined models for reactive transport of carbonated brine, geochemistry of reacting cement, and geomechanics to predict the permeability evolution of cement fractures. This addition makes the framework suitable for field conditions in geological storage sites, permitting simulation of contact between cement and mixtures of brine and supercritical CO_2.

Due to lack of conclusive experimental data, we tried both linear and Corey relative permeability models to simulate flow of the two phases in cement fractures. The model also includes two options to account for the inconsistent experimental observations regarding cement reactivity with two-phase CO_2-brine mixtures. One option assumes that the reactive surface area is independent of the brine saturation and the second option assumes that the reactive surface area is proportional to the brine saturation.

We have applied the model to predict the extent of cement alteration, the conditions under which fractures seal, the time it takes to seal a fracture, and the leakage rates of CO_2 and brine when damage zones in the wellbore are exposed to two-phase CO_2-brine mixtures. Initial brine residence time and the initial fracture aperture are critical parameters that affect the fracture sealing behavior. We also evaluated the importance of the model assumptions regarding relative permeability and cement reactivity. Our results illustrate the need to understand how mixtures of carbon dioxide and brine flow through fractures and react with cement to make reasonable predictions regarding well integrity. For example, a reduction in the cement reactivity with two-phase CO_2-brine mixture can not only significantly increase the sealing time for fractures but may also prevent fracture sealing.

1. Introduction

Depleted oil and gas reservoirs are prime candidates for injection of supercritical CO_2 for carbon dioxide storage (IPCC, 2005). However, sites with a history of oil and gas exploration and production activities typically contain abandoned wells, which may compromise the integrity of the storage site. While such abandoned wells are plugged with cement to prevent leakage, poor cement bonding or failure due to stresses (Zhang and Bachu, 2011; Nygaard et al., 2014) can create fractures in the cement, or at the cement-formation or cement-casing interfaces. These damage zones may allow carbon dioxide to leak from the reservoir, bringing single-phase and two-phase mixtures of supercritical/gaseous CO_2 and brine in contact with the wellbore cement. The purpose of this study is to understand the behavior of these multiphase mixtures and their interaction with wellbore cement.

Reactions between cement and carbonated brine alter cement's chemical, mechanical, and hydraulic properties. Under different circumstances these coupled processes can either hamper or even improve the cement's ability to seal the well. While several experiments have shown that reactions between CO_2-saturated brine and cement result in altered cement layers (Zhang and Bachu, 2011; Carey, 2013; Carroll et al., 2016), it is unclear how cement reacts with a two-phase mixture of brine and supercritical CO_2, or with brine-saturated supercritical CO_2 (*i.e.* "wet" supercritical CO_2). There have been insufficient experimental studies to determine how cement fractures respond to flows involving two-phase mixtures of brine and CO_2. Several batch experimental studies have attempted to characterize the interactions between cement and supercritical CO_2 but their results have been inconclusive. While some studies have shown that cement exposed to wet supercritical CO_2 results in the formation of reaction fronts within the cement (Barlet-

* Corresponding author at: L-286, 7000 East Avenue, Livermore, CA 94550, USA.
E-mail addresses: iyer5@llnl.gov (J. Iyer), stuart.walsh@unsw.edu.au (S.D.C. Walsh), hao1@llnl.gov (Y. Hao), carroll6@llnl.gov (S.A. Carroll).

https://doi.org/10.1016/j.ijggc.2017.12.001
Received 19 May 2017; Received in revised form 1 December 2017; Accepted 1 December 2017
Available online 08 January 2018

Gouédard et al., 2007; Rimmelé et al., 2008; Fabbri et al., 2009; Mito et al., 2015), others have observed uniform carbonation instead (Kutchko et al., 2008; Jung and Um, 2013). In the latter case, Kutchko et al. (2008) attributed the absence of reaction fronts to the lack of water. With regards to the rates of reactions, some studies showed no significant difference in the rate of alteration of cement upon exposure to carbonated brine or wet supercritical CO_2 (Barlet-Gouédard et al., 2007; Rimmelé et al., 2008; Lesti et al., 2013). Others have observed faster (Mito et al., 2015) or slower (Kutchko et al., 2008; Jung and Um, 2013) rates of alteration with wet supercritical CO_2 compared to carbonated brine. Kutchko et al. (2008) attributed the slow alteration rate with wet supercritical CO_2 to the lack of an aqueous phase to facilitate the diffusion of ions. Conversely, Mito et al. (2015) attributed the fast alteration rate with wet supercritical CO_2 to the lack of a diffusion barrier in the absence of water. In a different set of experiments, where wet and oven-dried cement samples were exposed to wet supercritical CO_2, Fabbri et al. (2009) showed that reaction fronts are present when wet cement in exposed to wet supercritical CO_2 and are absent when the cement was dried. They also found that the rate of degradation was lower in wet cement compared to dry cement, which they attributed to the diffusion barrier created by water in the wet cement. Although water plays a key role in the alteration of cement by carbon dioxide, the conflicting experimental observations make it difficult to identify the conditions under which water facilitates rather than inhibits these reactions. Differences in both the preparation and composition of cement samples, the details of which are often difficult to identify in the published literature, further muddles this issue.

It is essential to evaluate the behavior of mixtures of supercritical CO_2 and brine to accurately quantify the risk of carbon dioxide and brine leaking from a storage reservoir through damage in well cement. Differences in density, viscosity and relative permeability of the two phases have significant impacts on the flow rates of the individual phases in multiphase flow.

Over the last few years, we have developed an experimentally calibrated framework that couples reactive transport of carbonated brine, geochemistry of reacting cement, and geomechanics to predict the permeability evolution of leakage paths in cement exposed to carbonated brine (Walsh et al., 2013, 2014a,b; Iyer et al., 2017). In this paper, we extend our model to include two-phase flow of supercritical CO_2 and brine through leakage paths to make the model applicable to field conditions. We use the model to evaluate how two-phase flow impacts the chemical alteration of cement compared to carbonated brine. We also use the model to predict carbon dioxide and brine leakage rates through damage zones. The assumptions adopted for the relative permeability of CO_2 and brine flowing in fractures, and their reactivity with cement have a significant impact on the model's predictions. In light of the current lack of consensus regarding both of these factors, we investigate extremes in both cases in order to evaluate their impact on the chemical alteration of cement and the leakage rate of carbon dioxide and brine.

2. Model description

The present model builds on earlier work done to simulate the interaction between well cement and CO_2-saturated brine flowing through a fracture (Walsh et al., 2013, 2014a,b; Iyer et al., 2017). The original framework coupled a single-phase flow model for brine flow through a fracture, a reactive-transport model to predict the brine concentrations, a geochemical model for the CO_2-cement reactions, and a mechanical model to predict the change in fracture aperture due to the chemically altered cement. The models are implemented in the GEOS multi-physics framework developed at Lawrence Livermore National Laboratory (Settgast et al., 2017). Here, we describe how this framework can be extended to include a multiphase flow model to capture the flow of two-phase mixtures of brine and supercritical CO_2. We also describe the assumptions made with regards to the uncertainty surrounding (i) the relative permeability model for two-phase flow through fractures, and (ii) the impact of saturation on cement alteration rate.

2.1. Two-phase flow model

To model the two-phase flow of brine and carbon dioxide through a fracture, we first perform a mass balance for both brine and carbon dioxide. A depth-averaged mass balance for brine yields:

$$\frac{\partial}{\partial t}(b\rho_w\phi S_w) + \nabla\cdot(b\rho_w\mathbf{v}_w) = 0, \tag{1}$$

where the subscript w denotes the brine phase, b is the fracture aperture, ρ_i is the density of phase i, ϕ is the porosity of the medium, which is 1 in the case of a fracture, S_i is the saturation of phase i, and $\mathbf{v}_i$ is the superficial velocity of phase i. In this manuscript, our analysis is confined to one-dimensional flows for which the depth-averaged velocity vector can be represented as a scalar. Nevertheless, the approach and the code itself is applicable to flows through two-dimensional fractures, and consequently we leave the depth-averaged velocity as a vector. In addition, we have neglected the mass of brine diffusing in or out of the cement or solubilizing in the CO_2 phase, as these terms are expected to be significant only when the brine saturation is very low.

As carbon dioxide flows through the fracture, some of it is dissolved in the brine which subsequently diffuses into the cement and reacts with it. A mass balance of the carbon dioxide present in the CO_2 and the brine phases yields

$$\frac{\partial}{\partial t}\Big(b\phi(\rho_{g,w}S_w + \rho_g(1-S_w))\Big) + \nabla\cdot(b(\rho_{g,w}\mathbf{v}_w + \rho_g\mathbf{v}_g)) + R_C = 0, \tag{2}$$

where the subscript g denotes the CO_2 phase, $\rho_{g,w}$ is the solubility of carbon dioxide in the brine phase, and R_C is the rate at which carbon dioxide is consumed in the reactions with cement.

The velocities of the two phases in Eqs. (1) and (2) are calculated using the extension of Darcy's law for multiphase flow:

$$\mathbf{v}_i = -\frac{\mathrm{k}\mathrm{k}_{r,i}}{\mu_i}(\nabla p_i - \rho_i\mathbf{g}), \tag{3}$$

where the subscript i denotes the brine and CO_2 phases, k is the permeability of the fracture, $k_{r,i}$ is the relative permeability of phase i, μ_i is the viscosity of phase i, p_i is the pressure of phase i, and $\mathbf{g}$ is the gravity vector. As carbon dioxide and brine are immiscible, the two phases will have different pressures due to capillary forces:

$$p_w - p_g = \frac{2\gamma\cos\theta}{r_c}, \tag{4}$$

where the capillary pressure, $p_w - p_g$, is a function of the wetting angle θ, the surface tension between the phases γ, and the radius of curvature r_c. In a fracture the radius of curvature is well approximated as half the aperture ($r_c = b/2$), hence the smaller the aperture the larger the capillary pressure. Mixtures of supercritical CO_2 and brine have an interfacial tension of around 30 mN/m (Chalbaud et al., 2009). An aperture of 50 μm and a wetting angle of 30° (Saraji et al., 2013) gives a capillary pressure of 2 kPa. As we are applying this formulation to fractures with an aperture of 50–500 μm at average pressures around 10 MPa, we have assumed that the capillary pressure is small and have neglected it. Therefore, the pressure in both phases is the same and is denoted by p.

The permeability of the fracture in Eq. (3) is calculated using the following approximation (Witherspoon et al., 1980; Zimmerman and Bodvarsson, 1996):

$$k = \frac{b^2}{12}. \tag{5}$$

Modeling two phase flow in fractures is still an active area of research. In the microfluidics literature two-phase flow is modeled by

predicting the flow patterns observed at different flow conditions (Kawahara et al., 2002). However, in the earth science literature two-phase flow in fractures is modeled using the concept of relative permeability (Persoff and Pruess, 1995). In this manuscript we have also used relative permeability to describe two-phase flow in fractures. The relative permeability in Eq. (3) is a measure of the effective permeability of a phase in the presence of a second phase and varies between 0 and 1. It is typically modeled as a function of saturation. The simplest relative permeability model assumes that each phase does not interfere with the flow of the other and therefore, each phase's relative permeability is equal to its saturation:

$$k_{r,i} = S_{e,i}, \tag{6}$$

where $S_{e,i}$ is the effective saturation of phase i. The effective saturation is equal to

$$S_{e,i} = \frac{S_i - S_i^{\min}}{S_i^{\max} - S_i^{\min}}, \tag{7}$$

in which $S_i^{\max}$ and $S_i^{\min}$ are the maximum and minimum values of saturation for phase i calculated using the residual saturations of both phases. The above linear relative permeability model is based on the experimental work done by Romm and can over estimate the relative permeability of the phases (Persoff and Pruess, 1995). Other models have been developed based on the pore size distribution of the media (Bear, 1988). One such model developed by Corey (1954) is given by:

$$\begin{aligned} k_{r,\text{wet}} &= S_{e,\text{wet}}^4 \\ k_{r,\text{non-wet}} &= (1 - S_{e,\text{wet}})^2(1 - S_{e,\text{wet}}^2), \end{aligned} \tag{8}$$

where the subscripts *wet* and *non-wet* refer to the wetting and non-wetting phases, respectively. When using the Corey relative permeability model, we assume that brine is the wetting phase. There are several other relative permeability models which have been proposed for different material and fluid combinations.

It should be noted that relative permeability models have been primarily developed for three dimensional flows, in which it is possible to have two simultaneous percolating phases. This is not the case for two dimensional flows where in all but the most channelized flows only one percolating phase is possible. As a result, in two dimensions the two phases must change their configuration (through bubbles or changing connectivity) in order to flow. Thus, there is a question as to how applicable relative permeability models developed for three dimensional media are to fracture flows. Evidence also suggests that the actual form of the relative permeability is strongly influenced by both the fracture geometry and the applied pressure gradient (Walsh and Carroll, 2013). In the absence of experimental data or consensus on the relative permeabilities for two-phase mixtures of brine and carbon dioxide flowing through cement fractures, we have used both the linear and the Corey relative permeability models to understand their impact on the model predictions. As discussed in Walsh and Carroll (2013), while not perfect representations for two dimensional flows, relative permeability of wide fractures with high pressure gradients are bounded by the linear permeability model, while thin fractures with lower pressure gradients are better approximated by the Corey model (though greater phase interference can be observed in some cases). To improve model development, laboratory and field-scale studies that characterize CO_2-brine flow in cement fractures are essential.

Finally, to solve the two mass balances in Eqs. (1) and (2), models are required to calculate density, solubility, and viscosity as a function of pressure (in our calculations we have assumed the temperature to remain constant at 60 °C). The brine density and viscosity are calculated using the correlations developed by Phillips et al. (1981) for NaCl solutions. The molality of the brine, for the purpose of calculating its density and viscosity, is fixed at 1 m. The viscosity of pure water required for the brine viscosity calculations was obtained from the correlation developed by Meyer et al. (1968) (Miller, 1977). CO_2 viscosity was calculated using the equation developed by Fenghour et al. (1998). To simplify the CO_2 density calculations, we fitted a 4th order polynomial to density data at 60 °C and between 10 and 40 MPa obtained from the model by Span and Wagner (1996). The polynomial function and the coefficients are reported in Table S1 in the supplementary material. Similarly, to simplify the CO_2 solubility calculations, we fitted a 4th order polynomial to the solubility data for a 1 m NaCl solution at 60 °C and between 10 and 40 MPa obtained from the model by Duan and Sun (2003). The polynomial function and the associated coefficients are listed in Table S2 in the supplementary material.

Eqs. (1) and (2) are solved using a finite volume method to calculate the pressure and saturation along the fracture. This information is then used in Eq. (3) to calculate the velocities of the brine and CO_2 phases along the fracture.

To couple the two-phase flow model to the geochemical model, we need to calculate the concentrations of carbon and calcium along the fracture. It is assumed that the rate of solubilization (i.e. dissolution and speciation) of carbon dioxide in brine is significantly faster than the rate at which the aqueous carbon species react with the cement. Therefore, the carbon concentration in the brine is always fixed at its solubility and the rate at which carbon is consumed in the reaction with cement is accounted for in Eq. (2). To calculate the calcium concentration along the fracture, a mass balance on calcium is performed to get:

$$\frac{\partial}{\partial t}(bS_w[\text{Ca}]) + \nabla\cdot(b\mathbf{v}_w[\text{Ca}]) = \nabla\cdot(bS_w D\nabla[\text{Ca}]) - R_{\text{Ca}}, \tag{9}$$

where [Ca] is the depth-averaged calcium concentration, D is the diffusion coefficient, and $-R_{\text{Ca}}$ is the rate at which calcium is generated through the reactions between carbon and cement. We have assumed that the concentration gradient across the aperture of the fracture is negligible and therefore, Eq. (9) can be solved in 2-D. Once the carbon and calcium concentrations are known, they can be used by the geochemical model to evaluate the extent of reaction within the cement.

2.2. Geochemical model

The geochemical model used in this manuscript was developed by Walsh et al. (2013, 2014a,b) and Iyer et al. (2017). Only a brief description of the model is presented here and the details can be found in the original papers. The model is a “reduced physics” representation of the well-cement/carbonated-brine system. As acidic carbonated brine flowing in the fracture diffuses into the cement, it dissolves the portlandite present in cement to release calcium ions, which diffuse out of the cement. This results in the formation of a portlandite depleted layer within the cement. Inside the cement, where there is enough carbon and calcium, calcite precipitates to yield a calcite precipitate layer. If the calcium diffusing out of the cement is sufficient to saturate the carbonated brine in the fracture with respect to calcite, the calcite precipitate layer extends out of the cement into the fracture, and can potentially seal the damage zone (Huerta et al., 2016; Iyer et al., 2017). However, if there is insufficient calcium to saturate the brine outside the cement, then the calcite precipitate layer is confined within the cement, and an amorphous silicate layer (associated with the dissolution of other calcium phases) is formed next to the cement-brine interface.

To reduce the complexity of the model, Walsh et al. (2013) assumed that all reactions occur at the fronts between the altered layers and used a front tracking method to predict the progress of the reactions. We consider three distinct reaction fronts – following the geochemical model outlined by Kutchko et al. (2007).

- At the deepest front, Portlandite dissolution is assumed to occur at the interface between the unreacted cement and the portlandite depleted layer.

$$\text{Ca(OH)}_{2(s)} \rightarrow \text{Ca}^{2+} + 2\text{OH}^- \tag{10}$$

- Next, calcite precipitation is assumed to occur at the front between the portlandite depleted layer and calcite precipitate layer.

$$Ca^{2+} + CO_3^{2-} \rightarrow CaCO_{3(s)} \quad (11)$$

- Finally, calcite dissolution is assumed to occur at the front between the calcite precipitate layer and the amorphous silicate layer.

$$CaCO_{3(s)} \rightarrow Ca^{2+} + CO_3^{2-} \quad (12)$$

The calcite dissolution also coincides with the degradation of the cement's CSH-backbone, releasing additional calcium into the brine.

At each front we calculate the speciation of aqueous components under equilibrium conditions, considering equilibrium reactions associated with aqueous CO_2, H_2O, H^+, OH^-, H_2CO_3, HCO_3^-, CO_3^{2-}, Ca^{2+}, $CaHCO_3^+$, $CaCO_3$, $CaSO_4$, SO_4^{2-}, $CaCl_2$, $CaCl^+$, Cl^-, $MgSO_4$, Mg^{2+}, Na^+, and $NaSO_4^-$.

To model the movement of the fronts, the front velocity is related to the flux Q_E of an element E into (or out of) the front as follows:

$$Q_E = \frac{1}{\mathscr{M}_E}[[\rho_E(1-\phi)]]\frac{dx_I}{dt} = \Delta_E \frac{dx_I}{dt}, \quad (13)$$

where $[[A]] = A|_{x^+} - A|_{x^-}$ denotes the jump in a quantity A across the front, $\mathscr{M}_E$ is the molar mass of element E, ρ_E is the density of element E in the solid material, x_I is the front location, and Δ_E is the difference in the molar density of element E across the front.

The flux Q_E can be related to the rates of diffusion and reaction at the front. In prior work we have considered two limits (Walsh et al., 2013; Iyer et al., 2017). If the rate of reaction is significantly faster than the rate of diffusion, the reactions can be assumed to be at equilibrium. As a result, the concentration at the front is equal to the equilibrium concentration and Q_E can be calculated based on the diffusive flux to or from the front (Walsh et al., 2013). However, when the altered cement layers are very thin, the rate of diffusion can be faster than the rate of reaction. Due to the thin cement layers, the front concentration can be assumed to be equal to the brine concentration and Q_E can be written in terms of the rate of reaction at the brine conditions (Iyer et al., 2017). Thus, depending on which phenomenon is slower, the front concentration can be accordingly approximated and the front velocity can be calculated based on the rate of reaction or diffusion. The rates of consumption or generation of carbon and calcium used in Eqs. (2) and (9), respectively, can be calculated by summing the fluxes of carbon, Q_C, and calcium, Q_{Ca}, at each of the three fronts.

The geochemical model has to be coupled back to the flow model because the chemical alteration of the cement can change the permeability of the fracture. For example, precipitation of calcite within the fracture reduces the fracture aperture. To predict the permeability evolution of the fracture, the aperture obtained from the geochemical model is used to calculate the permeability using Eq. (5). This is subsequently used to calculate the pressure, saturation, and the velocity of the two phases along the fracture using Eqs. (1)–(3). The brine velocity is used to calculate the calcium concentration along the fracture using Eq. (9). This enables the reaction front model to update the locations of the reaction fronts and the value of the fracture aperture. Note that the fracture aperture can also decrease due to the mechanical deformation of the chemically altered cement (Walsh et al., 2014b). In this study we are primarily interested in understanding the effect of two-phase flow on the permeability evolution of cement fractures and have therefore, not included the effect of mechanical deformation.

A big uncertainty in modeling reactions between cement and carbon dioxide in two-phase systems is the role of water on the rate of reaction. As we have mentioned before, conflicting experimental observations in the literature make it difficult to identify the conditions under which the amount of water is too little to sustain the reactions or too much such that it creates a diffusion barrier. Water generated by the carbonation reaction might also play a role in the cement-CO_2 reactions. In the absence of clear experimental data, in this paper we consider two extremes. In the first case we assume that the rate of alteration of the cement remains the same irrespective of the saturation of the fluids flowing through the fracture. This condition tries to mimic the experimental findings of Barlet-Gouédard et al. (2007), Rimmelé et al. (2008); and Lesti et al. (2013) who found that the rates of alteration of cement upon exposure to carbonated brine or wet supercritical CO_2 were similar. In the second case, we assume that the amount of reactive surface area in the fracture is proportional to the brine saturation. As a result, the rate of alteration decreases as the brine saturation reduces. This would result in slower rates of alteration of the cement as reported by Kutchko et al. (2008) and Jung and Um (2013). However, unlike their experimental observations of uniform carbonation of cement, our model will still predict the formation of altered layers within the cement. Currently, we are unable to model the increase in the rate of alteration of cement due to the deeper penetration of the CO_2 phase within the cement (Mito et al., 2015) as we do not model advection of carbon dioxide or brine within the cement matrix.

3. Results and discussion

In this section, we use the model to assess the impact of two-phase flow on (i) the alteration within the cement and the fracture, and (ii) the risk of brine and carbon dioxide leakage. The effect of the choice of the relative permeability model and the assumption about cement's reactivity with the two-phase mixture is also evaluated. In addition, critical parameters that influence the sealing of cement fractures through calcite precipitation are determined.

Even though the model is capable of simulating 2-D flows through heterogeneous fractures, for the sake of simplicity, in this paper we confine our analysis to 1-D flows along fractures with a constant initial aperture. Unless otherwise noted the fractures have different apertures but are 1 m long and 20 mm wide. They are cement-cement fractures such that chemical reactions occur through both fracture surfaces. The values of the model parameters used in the simulations are reported in Table 1 in Iyer et al. (2017) and have been reproduced in Table S3 in the supplementary material. The concentrations of all the elements in brine, except carbon, are set equal to the values listed in Table 2 in Iyer et al. (2017) which are reproduced in Table S4 in the supplementary material. Finally, constant pressure drop boundary condition is used for all the simulations with a mean pressure along the fracture set equal to 12.4 MPa.

3.1. Impact of two-phase flow on cement alteration

In this section, we analyze how cement is altered when a two-phase mixture of supercritical CO_2 and brine flows through a cement–cement fracture. We use the model described above to predict the extent of cement alteration for both single-phase flow and two-phase flow through a fracture with an aperture of 100 μm. For the two-phase case, we compare the effects of both the linear and the Corey relative permeability models (the residual brine and carbon dioxide saturation are fixed at 0.01).

Fig. 1 shows the location of the three reaction fronts along the fracture after carbonated brine or a 50:50 two-phase mixture of carbon dioxide and brine have flown through the fracture for a day. Prior work by Iyer et al. (2017) and Brunet et al. (2016) showed that the brine flow rate strongly influences the interactions between cement and carbonated brine. Therefore, to compare similar scenarios, we adjusted the pressure drop for the simulations such that the initial brine flow rates are the same. To obtain an initial brine flow rate of 19.4 cc/min, the pressure drops for the single-phase, and two-phase flow simulations with the linear and Corey relative permeability models were set at

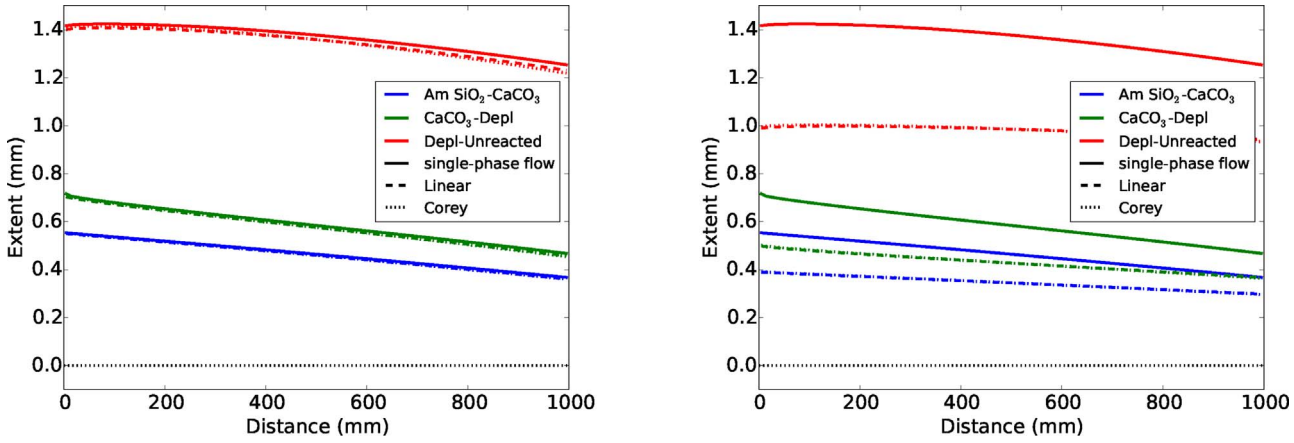

(a) Reactive surface area independent of saturation

(b) Reactive surface area proportional to brine saturation

Fig. 1. Model predictions of the front locations for single-phase and two-phase flow. In plot (a) the reactive surface area is independent of the saturation while in plot (b) the reactive surface area is proportional to the brine saturation. In both figures, the dashed black line indicates the initial location of the fracture surface. (For interpretation of the references to color in this figure, the reader is referred to the web version of this article).

0.1 MPa, 0.2 MPa, and 1.6 MPa, respectively. For the fracture dimensions mentioned before, this flow rate is sufficiently fast to prevent calcite precipitation within the fracture.

Fig. 1(a) shows that when the reaction rate is unaffected by brine saturation, the extent of alteration within the cement is almost identical for all three cases. This suggests that similar to the single-phase case, the extent of reaction within the cement predominantly depends on the brine flow rate for the two-phase case. Saturation and the relative permeability model impact the alteration through their effect on the brine flow rate. This conclusion does not hold when the reactive surface area, and therefore the reaction rate, is proportional to the brine saturation as shown in Fig. 1(b). For the same scenario, the extent of alteration is much lower for the two-phase flow simulation compared to the single-phase case. However, the extent of alteration is almost identical for the two relative permeability models. This is because both cases have the same brine saturation and therefore, the same reactive surface area. This suggests that if the reactive surface area is assumed to be proportional to the brine saturation, both the brine flow rate and the brine saturation affect the extent of alteration within the cement.

While the example in Fig. 1 corresponds to a flow rate that doesn't yield any precipitate within the fracture, similar conclusions are drawn for a flow rate that results in calcite precipitation within the fracture. This is shown in Section 3 in the supplementary material.

For single-phase flows of carbonated brine, it is possible to encounter scenarios in which calcite precipitate within the fracture is confined to the upstream end of the fracture (Huerta et al., 2016; Iyer et al., 2017). This occurs when the flow rate is sufficiently low that all of the carbon entering the fracture is precipitated as calcite in the upstream end of the fracture – preventing further reaction downstream. This is not the case for multiphase flow, because there is substantially more carbon per unit volume in supercritical CO_2 than in carbonated brine. With this virtually inexhaustible source of carbon, if the conditions are conducive for calcite precipitation, calcite will likely precipitate in a continuous layer as supercritical CO_2 flows all along the length of the fracture. This is shown in Fig. 2 which plots the reduction in the fracture aperture due to calcite precipitation within the fracture for both the single-phase and two-phase cases. The model predictions shown in Fig. 2 are for a 1 m long fracture with an aperture of 50 μm after 1 day. The initial brine flow rates for all three simulations in Fig. 2 were 0.01 cc/min. For the two-phase flow simulation, it was assumed that the reactive surface area is unaffected by the brine saturation. If the reactive surface area is instead assumed to be proportional to the brine saturation, then the amount of precipitate is reduced (as shown in Figure S1(d) in the supplementary material).

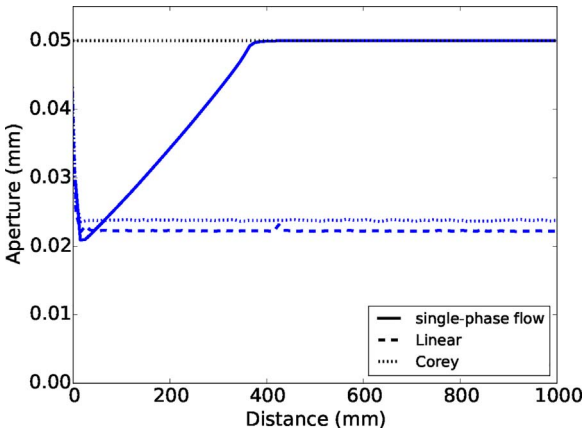

Fig. 2. Model predictions of the location of the calcite precipitate layer in the fracture for single-phase and two-phase simulations (using the linear and Corey relative permeability model). The dashed black line indicates the initial location of the fracture surface. (For interpretation of the references to color in this figure, the reader is referred to the web version of this article).

3.2. Critical parameters that determine fracture sealing

Work by Brunet et al. (2016) and Iyer et al. (2017) has shown that the initial brine residence time and fracture aperture are central to determining whether cement fractures exposed to carbonated brine will seal by calcite precipitation. The brine residence time is a measure of the average time required for brine to flow along the full length of the fracture. It is calculated as the ratio of the fracture volume and the average brine flow rate. Brunet et al. (2016) and Iyer et al. (2017) produced sealing maps that identified regions which show sealing and non-sealing behavior in fractures as a function of the initial fracture aperture and the initial brine residence time. In this section, we evaluate which variables play a key role in determining whether a fracture subjected to two-phase CO_2-brine flow will seal.

The initial brine residence time and fracture aperture remain as critical parameters in determining whether a fracture subjected to two-phase CO_2-brine flow will seal. This is concluded based on sealing maps constructed for both relative permeability models and several values of saturation. Fig. 3 shows two representative maps for a 1 m long cement fracture with an inlet brine saturation of 70%: Fig. 3(a) and (b) correspond to the linear and Corey relative permeability models, respectively. In both cases, it is assumed that the reactive surface area is

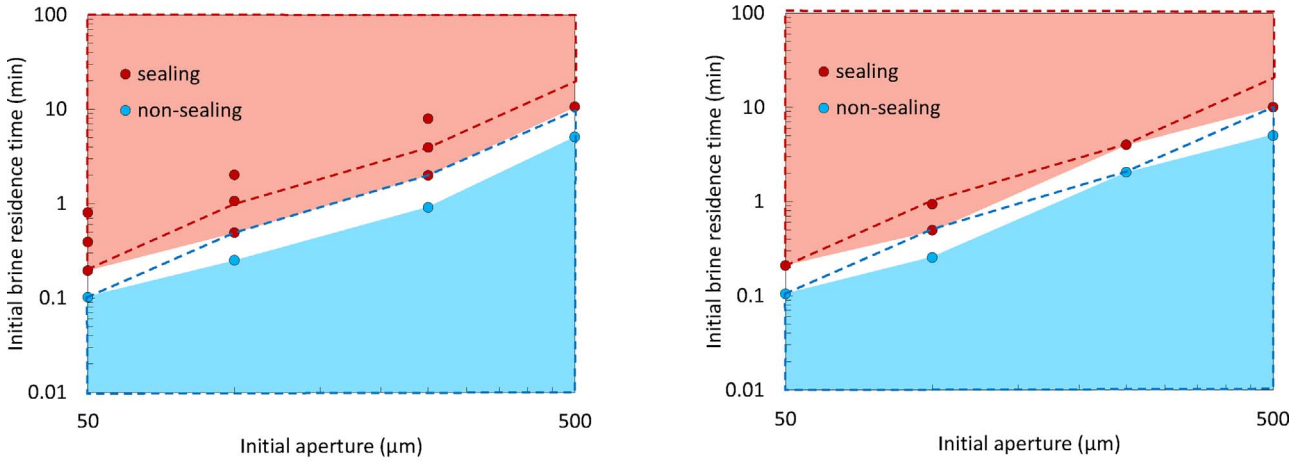

Fig. 3. Sealing map for two-phase flow showing regions of sealing and non-sealing behavior in fractures as a function of the initial fracture aperture and the initial brine residence time. Model predictions in plot (a) use the linear relative permeability model and in plot (b) use the Corey relative permeability model. It is assumed that the reactive surface area is unaffected by the brine saturation. The dashed lines denote the sealing and non-sealing regions obtained for single-phase flow (Iyer et al., 2017). (For interpretation of the references to color in this figure, the reader is referred to the web version of this article).

unaffected by the brine saturation. Changing the relative permeability model results in small changes on the sealing map. For two-phase flow the boundary between the sealing and non-sealing region moves to slightly lower initial brine residence times compared to the boundary for single-phase flow (dashed lines in Fig. 3). The slight downward movement of the boundary in the two-phase sealing maps results from the decease in fracture aperture and brine saturation due to calcite precipitation (see Section 3 and Figure S2 in the supplementary material). As a result, the reduction in brine flow rate in two-phase flow is larger than the reduction in brine flow rate in single-phase flow. This makes it slightly easier to seal the fracture with CO_2-brine mixtures than with carbonated brine when the reactive surface area is unaffected by brine saturation.

Like relative permeability, changing the initial brine saturation of the two-phase mixture does not significantly impact the sealing map when the reactive surface area is unaffected by brine saturation. Figure S3 illustrates this by comparing sealing maps developed for an inlet brine saturation of 20% and 70%.

It is important to note that the initial brine residence time, as a critical parameter, incorporates the effect of several modeling parameters including the inlet brine saturation and the relative permeability model. For a given pressure drop across a fracture, different relative permeability models and saturations can result in very different initial brine residence times. Consider a meter-long fracture with an aperture of 100 μm, subjected to a 70 kPa pressure drop and an inlet brine saturation of 0.7. The sealing map in Fig. 3 shows that the fracture would stay open if two-phase flow is governed by linear relative permeability (initial brine residence time = 0.24 min) and seal if flow is governed by Corey relative permeability (initial brine residence time = 0.7 min). Similarly, applying the same 70 kPa pressure drop while decreasing the inlet brine saturation to 0.2 increases the initial brine residence time from 0.24 min to 0.89 min when flow is governed by linear relative permeability. The longer residence time at lower brine saturation seals the fracture (see Figure S3). While the saturation and relative permeability model don't directly impact the sealing map significantly, they play a key role in determining the initial brine residence time, a major indicator of the likelihood that a fracture will seal.

The results discussed in Section 3.2 until this point have assumed that the reactive surface area is unaffected by the brine saturation. We also constructed sealing maps to understand the impact of the assumption that the reactive surface area is proportional to the brine saturation. As shown in Figs. 1(b), S1(b), and S1(d), coupling the reactive surface area to the brine saturation reduces the rate of alteration within the cement and the rate of calcite precipitation inside the fracture. This makes it harder to seal fractures by means of calcite precipitation. Therefore, longer residence times are required to seal fractures, and the boundary between the sealing and non-sealing regions moves to longer residence times when compared to the location of the boundary when the reactive surface area is unaffected by the brine saturation. The movement of the boundary increases as the brine saturation of the two-phase mixture decreases because a reduction in brine saturation decreases the amount of reactive surface. This is illustrated in Fig. 4 which shows the sealing map at 20% brine saturation for the two assumptions regarding the dependence of reactive surface area on brine saturation.

3.3. Leakage rates and sealing times

The sealing maps presented in the previous section provide information about the conditions under which a fracture will seal. It is equally important to know what leakage rates are expected from these

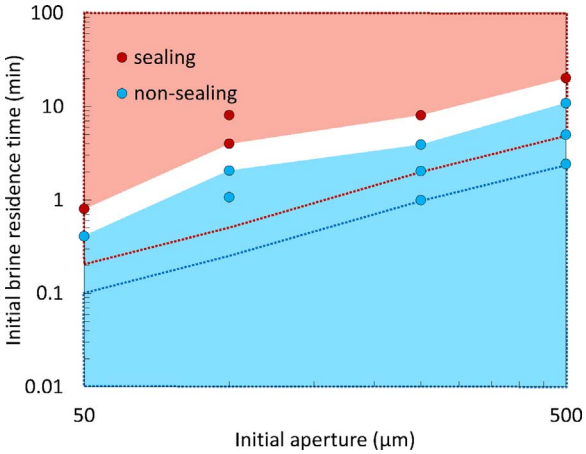

Fig. 4. Sealing map for two-phase flow with an inlet brine saturation of 20% and the assumption that the reactive surface area is proportional to the brine saturation. The dotted lines denote the sealing and non-sealing regions for an inlet brine saturation of 20% and when the reactive surface area is unaffected by the brine saturation. Both maps use the linear relative permeability model. (For interpretation of the references to color in this figure, the reader is referred to the web version of this article).

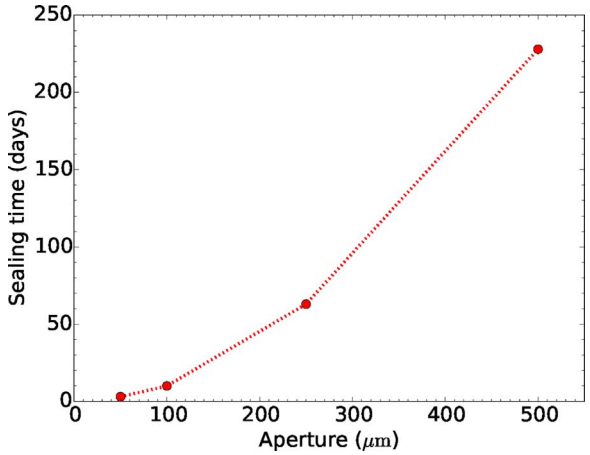

Fig. 5. Sealing time for fractures with different apertures. In all four simulations the reactive surface area is assumed to be independent of the brine saturation.

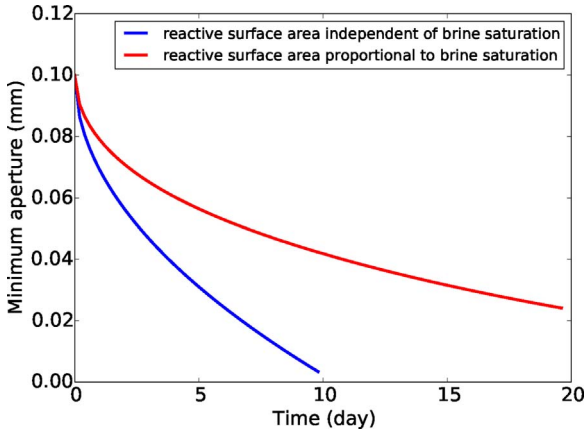

Fig. 6. Comparison between the sealing time of a 100 μm fracture when the reactive surface area is independent of the brine saturation and when the reactive surface area is proportional to the brine saturation. (For interpretation of the references to color in this figure, the reader is referred to the web version of this article).

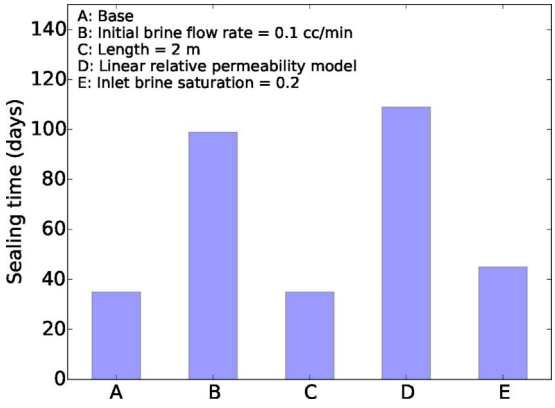

Fig. 7. Predicted sealing times for a 100 μm fracture when the reactive surface area is proportional to the brine saturation. The base case corresponds to an initial brine flow rate of 0.05 cc/min, length of 1 m, Corey relative permeability model, and an inlet brine saturation of 0.5. For the remainder four simulations all variables, except for the variable noted in the legend, were set equal to the values for the base case.

fractures and, for fractures that do seal, the length of time required. The sealing time for fractures can be defined in terms of reduction in leakage rates, permeability, aperture, etc. For simplicity, we defined the fracture sealing time as the time it takes for the minimum value of the fracture aperture along the length of the fracture to reduce to 1 μm. This is a reasonable definition when considering flow through 1-D fractures, because the effective permeability of a 1-D fracture is strongly affected by the minimum aperture along the fracture.

Since the amount of calcite precipitate required to seal a fracture will depend on the initial aperture of the fracture, it is expected that the sealing time has a strong dependence on the initial fracture aperture. In Fig. 5, the sealing times for 1 m long cement fractures subjected to flow of 50:50 mixtures of brine and carbon dioxide is plotted as a function of the initial fracture aperture. For all four simulations, we used the Corey relative permeability model, an initial brine residence time of 40 min, and a reactive surface area independent of the brine saturation. The sealing of fractures with a 250 and a 500 μm aperture were simulated for 50 and 120 days, respectively. The sealing times reported in Fig. 5 are extrapolations of the simulated data to a minimum aperture of 1 μm. Sealing times increase super-linearly with the initial fracture aperture. It takes significantly longer to seal larger apertures because thicker layers of calcite precipitate make it progressively more difficult for the dissolved ions to diffuse into the brine or cement to carry out the reactions.

The impact of other variables (*e.g.* fracture length, initial flow rate, inlet saturation, and relative permeability) were also considered. These variables have minimal impact on the sealing time when the reactive surface area is independent of saturation (see Section 5 in the supplementary material).

The sealing time is expected to increase substantially when we assume that the reactive surface area is proportional to the brine saturation due to the reduction in reaction rates. One such example is shown in Fig. 6 which compares the variation of the minimum aperture with time for a 100 μm fracture for the different reactive surface area assumptions. Extrapolating the red curve in Fig. 6 to a minimum aperture of 1 μm yields a sealing time of about 35 days for the case when the reactive surface area is proportional to brine saturation compared to 10 days when the reactive surface area is independent of saturation. This increase in sealing time becomes much more significant for larger fracture apertures which take much longer to seal as shown in Fig. 5.

Fig. 7 shows the impact of initial brine flow rate, fracture length, relative permeability model, and inlet saturation on the sealing time when the reactive surface area is proportional to the brine saturation. All of these variables influence how the brine saturation along the fracture changes with time; which in turn directly affects the rate of calcite precipitation because the reactive surface area is proportional to the brine saturation. Thus, these variables have a substantial effect on the sealing time. When the reactive surface area is independent of saturation, even though these variables affect saturation, they do not change the rate of calcite precipitation and the time needed to seal the fracture (see Section 5 in the Supplementary material).

In Fig. 8 we plot the brine and CO_2 leakage rates for a meter-long fracture with an aperture of 100 μm and a width of 20 mm, subjected to a 14 kPa pressure drop. In this example, CO_2 leakage rate is significantly higher (~50 times) than brine leakage rate, despite the inlet saturation being 0.5. As the fracture seals, the brine leakage rate drops faster than the CO_2 leakage rate. This is because the denser and more viscous brine finds it difficult to flow against gravity as the permeability of the fracture decreases. While Fig. 8 only shows one example, these trends are expected for other operating conditions as well in which two-phase mixtures of brine and carbon dioxide leak through sealing cement fractures. The quantitative values of the leakage rates will depend not only on whether the reactive surface area is affected by saturation, but also on the length, aperture, and width of the fracture, the pressure drop across the fracture, the saturation of the two-phase mixture, and the relative permeability model. Fig. 8 illustrates how incorporating a two-phase flow model in our coupled framework allows us to predict both the brine and CO_2 leakage rates that are important to assess the leakage risk from a storage site.

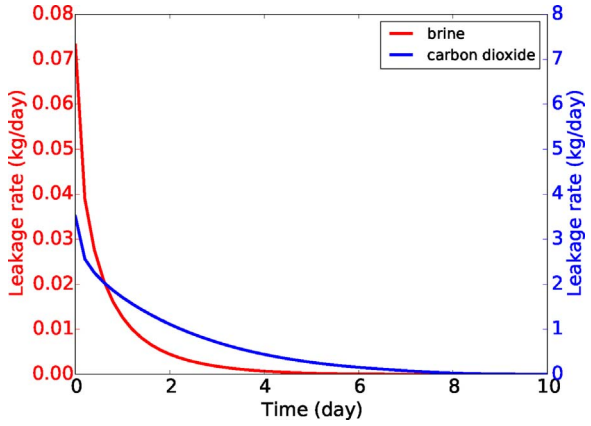

Fig. 8. Brine and CO_2 leakage rates. (For interpretation of the references to color in this figure, the reader is referred to the web version of this article).

4. Conclusions

While reaction of cement with carbon dioxide is predominantly mediated by brine, modeling of two-phase flow is necessary to accurately estimate brine and CO_2 leakage rates. In this paper, we have coupled a model for two-phase flow of CO_2-brine mixtures to our original numerical framework that combined models of reactive transport of carbonated brine, geochemistry of reacting cement, and geomechanics to predict the permeability evolution of cement fractures exposed to carbonated brine. This addition makes the framework more broadly suited to model field conditions in underground storage sites, which are expected to comprise supercritical CO_2-brine mixtures.

To model two-phase flow through fractures, we used the extension of Darcy's law for multiphase flow to compute the transmission of the brine and CO_2 phases. In the absence of academic consensus on the relative permeability of the two fluids in cement fractures, we have used the linear and Corey relative permeability models in our calculations. In addition, due to conflicting data regarding the effect of supercritical CO_2 on the rate of alteration of cement, we compared the results of modeling two extreme scenarios: (i) reactive surface area is independent of the saturation of the two-phase mixture; (ii) reactive surface area is proportional to the brine saturation.

Our model predictions for 1-D fractures show that if the rate of alteration of cement is assumed to be independent of the saturation of the two-phase mixture then the extent of reaction within the cement and in the fracture is similar for both single and two-phase flow as long as the initial brine flow rate is the same. The saturation and relative permeability model affect the extent of cement alteration through their effect on the brine flow rate.

Results from our model demonstrate that the initial brine residence time and the initial fracture aperture are critical parameters that determine whether a fracture, subjected to two-phase flow, would seal. This conclusion is also identical to that drawn for single-phase flow (Brunet et al., 2016; Iyer et al., 2017). While the direct impact of relative permeability models and saturation on the sealing map were small, both variables are extremely important to determine the brine residence time for a given pressure condition. Thus, it is necessary to understand which relative permeability model describes the flow of carbon dioxide and brine through cement fractures to make reasonable predictions about the permeability evolution of these fractures.

Significant differences were observed between two-phase and single-phase flow when the reactive surface area was assumed to be proportional to the brine saturation. Reduced surface areas led to reduced alteration within the cement and inside the fracture for two-phase flow, requiring longer residence times to seal fractures. This highlights the necessity of understanding the reactivity of CO_2-brine mixtures with cement, as their reactivity can greatly influence the sealing of the fluid pathway.

For fractures that were observed to seal, we presented model predictions of sealing times and leakage rates. The sealing times were significantly longer when the reactive surface area is proportional to the brine saturation compared to when the reactive surface area is independent of saturation. When the reactive surface area is independent of the brine saturation, the sealing time was primarily influenced by the initial fracture aperture. The impact of other variables like fracture length, flow rate, saturation, and relative permeability was insignificant. However, all these variables have a significant impact on the sealing time when the reactive surface area is assumed to be proportional to the brine saturation.

Critical output from any well integrity model includes CO_2 and brine leakage rates to evaluate the impact on underground drinking water sources or the atmosphere. CO_2 leakage rates can be significantly higher than brine leakage rates due to its lower density and viscosity compared to brine. Moreover, these rates can change depending on the saturation conditions and the relative permeability model used to model two-phase flow. Thus, even though the reactions between carbon dioxide and cement are mediated by brine, it is imperative to model the supercritical CO_2 phase as well, to accurately quantify the leakage risk of carbon dioxide.

Acknowledgements

This work was performed under the auspices of the U.S. Department of Energy by Lawrence Livermore National Laboratory under Contract DE-AC52-07NA27344. This work was completed as part of the National Risk Assessment Partnership (NRAP) project. Support for this project came from the DOE Office of Fossil Energy's Carbon Capture and Storage program. The authors wish to acknowledge Traci Rodosta (NETL Carbon Storage Program) and Mark Ackiewicz (DOE Office of Fossil Energy) for programmatic guidance, direction, and support. In addition, a part of this work was conducted using resources provided by the Pawsey Supercomputing Centre with funding from the Australian Government and the Government of Western Australia.

Appendix A. Supplementary data

Supplementary data associated with this article can be found, in the online version, at https://doi.org/10.1016/j.ijggc.2017.12.001.

References

Barlet-Gouédard, V., Rimmelé, G., Goffé, B., Porcherie, O., 2007. Well technologies for CO_2 geological storage: CO_2-resistant cement. Oil Gas Sci. Technol. – Rev. I'IFP 62, 325–334.
Bear, J., 1988. Dynamics of Fluids in Porous Media. Dover Publications, pp. 459–466.
Brunet, J.P.L., Li, L., Karpyn, Z.T., Huerta, N.J., 2016. Fracture opening or self-sealing: critical residence time as a unifying parameter for cement-CO_2-brine interactions. Int. J. Greenh. Gas Control 47, 25–37.
Carey, J.W., 2013. Geochemistry of wellbore integrity in CO_2 sequestration: Portland cement-steel-brine-CO_2 interactions. Rev. Mineral. Geochem. 77, 505–539.
Carroll, S., Carey, J.W., Dzombak, D., Huerta, N.J., Li, L., Richard, T., Um, W., Walsh, S.D.C., Zhang, L., 2016. Review: Role of chemistry, mechanics, and transport on well integrity in CO_2 storage environments. Int. J. Greenh. Gas Control 49, 149–160.
Chalbaud, C., Robin, M., Lombard, J.M., Martin, F., Egermann, P., Bertin, H., 2009. Interfacial tension measurements and wettability evaluation for geological CO_2 storage. Adv. Water Resour. 32, 98–109.
Corey, A.T., 1954. The interrelation between gas and oil relative permeabilities. Prod. Mon. 19, 38–41.
Duan, Z., Sun, R., 2003. An improved model calculating CO_2 solubility in pure water and aqueous NaCl solutions from 273 to 533 K and from 0 to 2000 bar. Chem. Geol. 193, 257–271.
Fabbri, A., Corvisier, J., Schubnel, A., Brunet, F., Goffé, B., Rimmele, G., Barlet-Gouédard, V., 2009. Effect of carbonation on the hydro-mechanical properties of Portland cement. Cem. Concr. Res. 39, 1156–1163.
Fenghour, A., Wakeham, W.A., Vesovic, V., 1998. The viscosity of carbon dioxide. J. Phys. Chem. Ref. Data 27, 31–44.
Huerta, N.J., Hesse, M.A., Bryant, S.L., Strazisar, B.R., Lopano, C., 2016. Reactive transport of CO_2-saturated water in a cement fracture: application to wellbore

leakage during geologic CO_2 storage. Int. J. Greenh. Gas Control 44, 276–289.
IPCC, 2005. In: Metz, B., Davidson, O., de Coninck, H.C., Loos, M., Meyer, L.A. (Eds.), IPCC special report on carbon dioxide capture and storage. Prepared by working group III of the intergovernmental panel on climate change. Cambridge University Press, Cambridge, United Kingdom and New York, NY, USA, pp. 213–225.
Iyer, J., Walsh, S.D.C., Hao, Y., Carroll, S.A., 2017. Incorporating reaction-rate dependence in reaction-front models of wellbore-cement/carbonated-brine systems. Int. J. Greenh. Gas Control 59, 160–171.
Jung, H.B., Um, W., 2013. Experimental study of potential wellbore cement carbonation by various phases of carbon dioxide during geologic carbon sequestration. Appl. Geochem. 35, 161–172.
Kawahara, A., Chung, P.M.Y., Kawaji, M., 2002. Investigation of two-phase flow pattern, void fraction and pressure drop in a microchannel. Int. J. Multiph. Flow 28, 1411–1435.
Kutchko, B.G., Strazisar, B.R., Dzombak, D.A., Lowry, G.V., Thaulow, N., 2007. Degradation of well cement by CO_2 under geologic sequestration conditions. Environ. Sci. Technol. 41, 4787–4792.
Kutchko, B.G., Strazisar, B.R., Lowry, G.V., Dzombak, D.A., Thaulow, N., 2008. Rate of CO_2 attack on hydrated class H well cement under geologic sequestration conditions. Environ. Sci. Technol. 42, 6237–6242.
Lesti, M., Tiemeyer, C., Plank, J., 2013. CO_2 stability of Portland cement based well cementing systems for use on carbon capture and storage (CCS) wells. Cem. Concr. Res. 45, 45–54.
Meyer, C.A., McClintock, R.B., Silvestri, G.J., Spencer, R.C., 1968. 1967 ASME Steam Tables: Thermodynamic and Transport Properties of Steam. American Society of Mechanical Engineers, New York.
Miller, R.E., 1977. A Galerkin, finite-element analysis of steady-state flow and heat transport in the shallow hydrothermal system in the East Mesa area, Imperial Valley, California. J. Res. U.S. Geol. Surv. 5, 497–508.
Mito, S., Xue, Z., Satoh, H., 2015. Experimental assessment of well integrity for CO_2 geological storage: batch experimental results on geochemical interactions between a CO_2-brine mixture and a sandstone-cement-steel sample. Int. J. Greenh. Gas Control 39, 420–431.
Nygaard, R., Salehi, S., Weideman, B., Lavoie, R.G., 2014. Effect of dynamic loading on wellbore leakage for the Wabamun area CO_2-sequestration project. J. Can. Petrol. Technol. 53, 69–82.
Persoff, P., Pruess, K., 1995. Two-phase flow visualization and relative permeability measurement in natural rough-walled rock fractures. Water Resour. Res. 31, 1175–1186.
Phillips, S.L., Igbene, A., Fair, J.A., Ozbek, H., Tavana, M., 1981. A Technical Databook for Geothermal Energy Utilization. Lawrence Berkeley Laboratory, University of California, Berkeley, pp. 14–15.
Rimmelé, G., Barlet-Gouédard, V., Porcherie, O., Goffé, B., Brunet, F., 2008. Heterogeneous porosity distribution in Portland cement exposed to CO_2-rich fluids. Cem. Concr. Res. 38, 1038–1048.
Saraji, S., Goual, L., Piri, M., Plancher, H., 2013. Wettability of supercritical carbon dioxide/water/quartz systems: simultaneous measurement of contact angle and interfacial tension at reservoir conditions. Langmuir 29, 6856–6866.
Settgast, R.R., Fu, P., Walsh, S.D.C., White, J.A., Annavarapu, C., Ryerson, F.J., 2017. A fully coupled method for massively parallel simulation of hydraulically driven fractures in 3-dimensions. Int. J. Numer. Anal. Methods Geomech. 41, 627–653.
Span, R., Wagner, W., 1996. A new equation of state for carbon dioxide covering the fluid region from the triple-point temperature to 1100 K at pressures up to 800 MPa. J. Phys. Chem. Ref. Data 25, 1509–1596.
Walsh, S.D.C., Carroll, S.A., 2013. Fracture-scale model of immiscible fluid flow. Phys. Rev. E 87, 013012.
Walsh, S.D.C., Frane, W.L.D., Mason, H.E., Carroll, S.A., 2013. Permeability of wellbore-cement fractures following degradation by carbonated brine. Rock Mech. Rock Eng. 46, 455–464.
Walsh, S.D.C., Mason, H.E., Frane, W.L.D., Carroll, S.A., 2014a. Experimental calibration of a numerical model describing the alteration of cement/caprock interfaces by carbonated brine. Int. J. Greenh. Gas Control 22, 176–188.
Walsh, S.D.C., Mason, H.E., Frane, W.L.D., Carroll, S.A., 2014b. Mechanical and hydraulic coupling in cement-caprock interfaces exposed to carbonated brine. Int. J. Greenh. Gas Control 25, 109–120.
Witherspoon, P.A., Wang, J.S.Y., Iwai, K., Gale, J.E., 1980. Validity of cubic law for fluid flow in a deformable rock fracture. Water Resour. Res. 16, 1016–1024.
Zhang, M., Bachu, S., 2011. Review of integrity of existing wells in relation to CO_2 geological storage: what do we know? Int. J. Greenh. Gas Control 5, 826–840.
Zimmerman, R.W., Bodvarsson, G.S., 1996. Hydraulic conductivity of rock fractures. Transp. Porous Media 23, 1–30.